

# Characterization of phase transitions on $\text{PbZr}_x\text{Ti}_{(1-x)}\text{O}_3$ nanocrystal ceramic materials synthesized using the molten salt method

 Syahfandi Ahda <sup>a,\*</sup>, Laras Zulhijah <sup>b</sup>, Noviyan Darmawan <sup>b</sup>, Arbi Dymiati <sup>a</sup>
<sup>a</sup> Center for Science Technology of Advanced Materials, National Nuclear Energy Agency, Indonesia

<sup>b</sup> Chemistry Department, Bogor Agricultural Institute, Indonesia

\* Corresponding author: idnafahda@gmail.com

## Article history

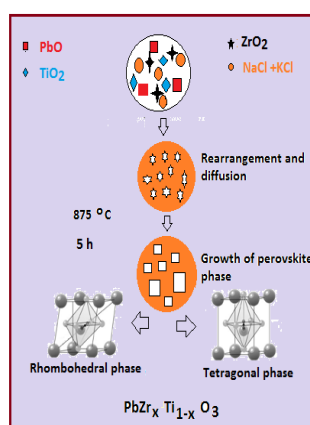
Received 30 January 2019

Revised 18 Mac 2019

Accepted 1 October 2019

Published Online 3 December 2019

### MOLTEN SALT METHOD



## Abstract

One of the piezoelectric materials is  $\text{PbZr}_x\text{Ti}_{(1-x)}\text{O}_3$  (Lead Zirconate Titanate, namely PZT) which has the highest piezoelectric properties and is widely applied today. To improve the performance of materials, it is important to enhance the quality of materials, especially in the synthesis process. In this study, molten salt method was employed to synthesis PZT by using salt solution ( $\text{NaCl}$  and  $\text{KCl}$ ) in accommodating the reaction of raw materials ( $\text{Pb}$ ,  $\text{ZrO}_2$ , and  $\text{TiO}_2$ ). The synthesized particles of PZT nanocrystal ceramics have been successfully carried out at the sintering temperature of  $875\text{ }^\circ\text{C}$  for 4 hours. The separations of  $\text{NaCl}$  and  $\text{KCl}$  salt to obtain PZT products have been carried out by washing repeatedly with hot water at about  $100\text{ }^\circ\text{C}$ .  $\text{PbZr}_x\text{Ti}_{(1-x)}\text{O}_3$  samples with variations of  $x = 0.30, 0.42, 0.52, 0.58,$  and  $0.70$  mol were characterized using X-Ray Diffractometer and followed by analyzing crystal structures using highscore software through refinement process. One of the X-ray diffraction profiles at the angle ( $2\theta$ ) between  $42.5$  and  $47^\circ$  has indicated the phase transition from one peak (representing the rhombohedral crystal system with the plane (202)) to the two peaks (tetragonal with plane (002) and (200)). Regarding this phase transition, the morphotropic phase boundary (MPB) region (rhombohedral and tetragonal phase boundary region) has been successfully obtained at the composition  $x = 0.52$  mol which was identical to the  $\text{PbZr}_{0.52}\text{Ti}_{0.48}\text{O}_3$  compound. The largest particle size of crystallites for each rhombohedral and tetragonal phase is approximately equal to  $906.117\text{ \AA}$  obtained at the composition  $x = 0.52$  mol. The content of the rhombohedral phase decreases, while the content of the tetragonal phase increases if the value of  $x$  increases.

**Keywords:** Molten salt method, Morphotropic Phase Boundary (MPB)

© 2019 Penerbit UTM Press. All rights reserved

## INTRODUCTION

The solid solution  $\text{PbZr}_x\text{Ti}_{1-x}\text{O}_3$ , labeled as lead zirconate titanate (PZT), is one of the most popular and widely studied or applied materials in the last decade, due to its excellent dielectric, ferroelectric, and piezoelectric properties. Many researchers have attempted to synthesize PZT for various compositions and methods and also followed by studying the crystalline structure system that was formed. The highest piezoelectric coefficient of PZT was found at compositions close to the morphotropic phase boundary (MPB), between the tetragonal and rhombohedral borders, as shown in the temperature-composition phase diagram [1-2].

Generally, the PZT materials are synthesized by a solid-state reaction with use of the starting material of  $\text{PbO}$ ,  $\text{TiO}_2$ , and  $\text{ZrO}_2$  (the usual dry method) in which this reaction sequence is well known now, and some studies illustrate it very well [3-4]. In this synthesis process is generally to apply high temperature with a long time, so high financing is required. To overcome this problem, a low-temperature synthesis route becomes a choice to be adapted and used. Various examples of methods in the production of low-temperature ceramic powders to produce piezoelectric ceramic, especially for  $\text{K}_{1/2}\text{Nb}_{1/2}\text{NbO}_3$  and  $\text{BaTiO}_3$  as examples, including the

synthesis of molten salt (MSS) [5-6], citrate method [7], sol-gel method [8], a hydrothermal process [9].

Among these methods, MSS exceptionally provides low cost, simplicity [10], resilience, and easy for effective improvement. When compared to conventional synthesis for mixed oxides, the MSS is one that can represent low-temperature routes for these improvements.

In principle, the MSS method uses molten salt as a medium for the manufacture of complex oxides of its constituents (oxides and carbonates). In this case, reaction mechanism in the MSS is a little different from the solid-state reaction, due to the absence of the sample compaction, as long as the salt mixed in a reaction formation. The molten salt in this method is a modification of a conventional powder metallurgy method. In the synthesis process, salt (consisting of  $\text{NaCl} + \text{KCl}$ , low melting point) can be put into reactants and reheated above the melting point of the salt. The expected compound will be formed if it is thermodynamically more stable than the constituent oxide and this stability is based on more than simple entropy of mixing. The function of solvents in large amounts of salt is to control the characteristics of the powder, such as size, shape and others. This method also uses salt as an additive or catalyst to increase the reaction rate and is different from the flux method [11-12].

In the present study, a molten salt method was applied for the synthesis of PZT piezoelectric nanoparticles in various compositions. It can be expected to determine the boundary region, known as MPB, between two kinds of crystalline systems of rhombohedral and tetragonal. In addition, the synthesized PZT material has been characterized using x-ray diffraction methods to determine the crystalline system and crystallite particle size with variations in the composition of  $x$  in PZT.

## EXPERIMENTAL

High-purity commercial PbO (Merck Co., 99.5 %), ZrO<sub>2</sub> (Merck, 99.9 %) and TiO<sub>2</sub> (Merck Co., 99.5 %) were used as starting materials, whereas NaCl (Merck Co., 99.0 %) and KCl (Merck Co., 99.0 %) were used as salt medium on molten salt method. While the prepared samples were expected to form the compounds of PbZr<sub>x</sub>Ti<sub>(1-x)</sub>O<sub>3</sub>, the value of  $x$  was varied at 0.3, 0.48, 0.52, 0.58, and 0.7. At the beginning the starting materials of PbO, ZrO<sub>2</sub> and TiO<sub>2</sub> were weighed in stoichiometry and continued with grinding using the agate mortar for 2 hours. NaCl and KCl salts (1:1 mole ratio) were mixed into the ground starting materials with a weight ratio of 1:1 and then continued to grind for 2 hours. During grinding, the mixture was expected to be homogeneously mixed and particle size was getting smaller. The mixtures were heated in a high-purity alumina crucible at the temperature 875 °C for 4 hours.

The schematic of the synthesis process is shown in the Fig. 1.

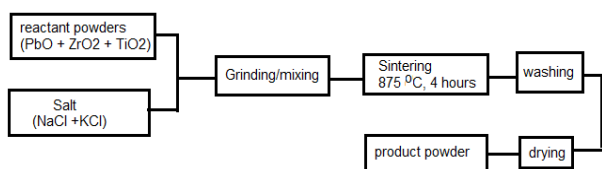


Fig. 1 Schematic of synthesis process using molten salt method.

In order to remove the salt contents after sintering, the mixture were washed thoroughly with hot water. The presence of salt were observed by dropping AgNO<sub>3</sub> solution into the filtered water (purple color and colorless indicate the existence and absence of salt, respectively). This process has been continued by heating the sample around 100 °C, in order to remove water during the washing. Finally, The characterization and identification of powder samples by using the x-ray diffraction machine for powder samples has been carried out. Analysis of crystal system for each sample has been done by Rietveld refinement process using the Highscore Rietveld program.

## RESULTS AND DISCUSSION

X-ray diffraction (XRD) patterns were recorded for characterization at room temperature using a PW1710 type PANalytical EMPYREAN XRD machine by employing CuK $\alpha$  radiation. Some of these XRD patterns recorded for some compounds (as an example) are shown in the figure below. Fig. 2 shows x-ray diffraction (XRD) patterns of the starting materials and also the synthesized PZT. Each starting material has the 3 highest peaks, as shown on PbO at the diffraction angle (with its  $2\theta$ ) of 29.22, 56.14 and 30.48°, ZrO<sub>2</sub> at 28.28, 31.56 and 50.18°, and TiO<sub>2</sub> 25.40, 48.10 and 37.86°. However, the absence of the three highest peaks (as well as Hanawalt identification) of each starting material on PZT pattern has represented that the synthesis process has been successfully performed. Similarly, the XRD profile of the salt materials does not exist in the synthesis product, it means that all the salt materials can be separated in the washing process. The XRD pattern of PZT show the sharp diffraction peaks, which indicates a better homogeneity and crystallization of the samples [13].

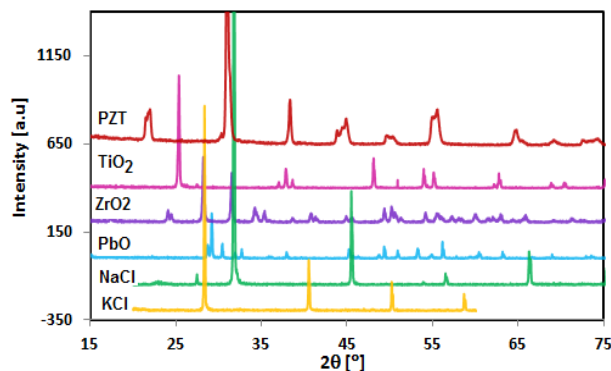


Fig. 2 X-ray diffraction patterns of synthesis product (PZT), the starting materials (PbO, ZrO<sub>2</sub> and TiO<sub>2</sub>) and salt (NaCl and KCl).

In the application of the molten salt method, the synthesis process was carried out by varying the value of  $x$  (0.7, 0.58, 0.52, 0.48, and 0.3 mol) on products of PbZr<sub>x</sub>Ti<sub>(1-x)</sub>O<sub>3</sub> and obtained the new compounds with characteristics of different diffraction patterns.

For further analysis, the study of phases and crystal systems presented in the material is an important parameter for controlling or identifying microstructures and the correlation properties associated with the synthesis process stage, in particular, the molten salt method. The analysis of the diffraction patterns of these synthesized products is shown in Fig. 3. Patterns of the sintered PZT ceramics at 875 °C for 4 hours in molten salt indicate co-existence of the rhombohedral and tetragonal phases. The result shows a change of peak at 2 thetas of around 21.5 and 44.5° from one to two peaks (like splitting) when the value of  $x$  is varied from 0.7 to 0.3 mole. In this case, there has been a change of phase clearly indicating the presence of the rhombohedral (JCPDS 73-202) and tetragonal phase (33-0784), as shown in the same study on Si<sub>3</sub>N<sub>4</sub> by Orapim Namsar [14].

All XRD diffraction patterns for synthesis products have been refined using the Highscore Rietveld program (version 4.7.0) with the pseudo-Voigt profile function in all cases. The Rietveld method has involved the refinement of the crystal structure by using data from an X-ray source with a powder sample. At the same time the Rietveld program also allows refining cell units, microstructure, quantitative phase analysis, and determination of the preferred orientation.

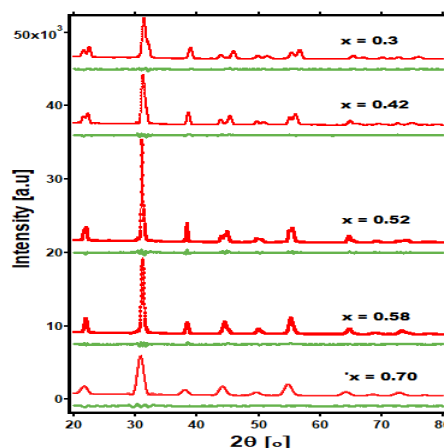


Fig.3 X-ray diffraction patterns and refinement results of PbZr<sub>x</sub>Ti<sub>(1-x)</sub>O<sub>3</sub> materials ( $x= 0.7, 0.58, 0.52, 0.42,$  and  $0.3$ ). The red point sign (•) is the intensity of observation ( $I_{obs}$ ), red line (—,  $I_{cal}$ ) is calculation intensity, green line (—, diff) is the intensity difference between  $I_{obs}$  and  $I_{cal}$ .

Therefore, all samples with different compositions have been refined using 2 kinds of space groups of P4mm representing the tetragonal and R3c representing the rhombohedral in perovskite crystal system, as indicated by the refinement results in Fig. 3. The initial refinement process was done by the zero-point shift, background and the unit-cell parameters. The evolution of the unit cell parameters as a function of composition  $x$  reveals rhombohedral

to tetragonal phase transition (with the splitting or overlapping of the peaks).

The quality of the fittings can be verified by two numerical statistical indicators of  $R_e$  and  $R_{wp}$  and make the comparative parameters between theoretical and experimental XRD patterns, which can be used to monitor the convergence of models. The final results of this refinement are shown in Table 1. The weighted R-factors of ( $R_{wp}$ ) and the expected R -factor ( $R_{exp}$ ) of less than 5.3 % have shown good agreement results in the fit process. This can be shown also in that the difference in intensity between observation and calculation (green) is relatively very low which indicates a good agreement in this refinement process.

**Table 1** Crystal structure parameters for  $PbZr_xTi_{1-x}O_3$  (PZT) obtained from the refinement process using X-ray powder diffraction data at room temperature.

x [mol]	Tetragonal		Rhombohedral		$R_e$ [%]	$R_{wp}$ [%]
	a=b [Å], c [Å]	c/a	a=b=c [Å]	= [%]		
0.3	3.9517, 4.1222	1.043			3.916	4.807
0.42	3.9997, 4.1324	1.033	4.0414	89.98	3.889	5.162
0.52	4.0353, 4.1301	1.023	4.0754	90.01	3.689	5.343
0.58	4.0325, 4.1301	1.024	4.0858	89.82	3.788	5.080
0.7			4.1043	89.73	3.554	4.813

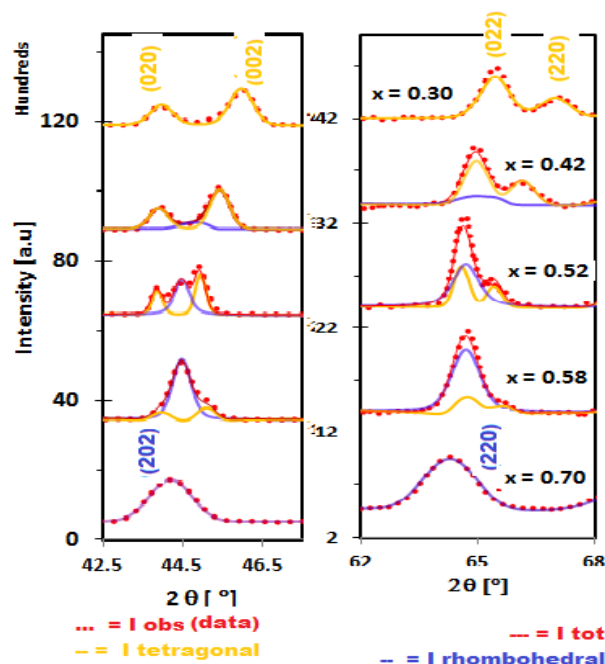
The  $R_{wp}$  value for a good fitting process should be 2-10% to be considered as an acceptable model, as suggested by Knies et al. [15-16].

Table 1 shows variations of lattice parameters 'a' and 'c' and 'c/a' ratio as a function of x moles of  $PbZr_xTi_{(1-x)}O_3$  ceramic powder. The minimum ratio of 1.023 has been found at  $x = 0.52$  mol and also the constant lattice 'c' is the constant for the addition of x from 0.52 to 0.58 mol. This decrease in c/a ratio indicates that the PZT ceramic tetragonality decreases with increasing Zr content. Therefore the phase transition (tetragonal to rhombohedral) is strongly possible to occur at the ratio  $Zr/Ti = 0.52 / 0.48$ , as has been done also by Karapuzha [17].

For more details of the 2-phase existence, we can analyze the peaks at the diffraction angles ( $2\theta$ ) of between  $42.5-47^\circ$  and  $62-68^\circ$ , as can be shown in the Fig. 4 for various compound compositions labeled with x. A peak represented in the (202) rhombohedral plane has transformed into two peaks represented in the (020) and (002) tetragonal plane for the diffraction angle between  $42.5-47^\circ$ . Similarly, the rhombohedral (220) plane becomes the plane (022) and (220) tetragonal for the angle ( $2\theta$ ) between  $62-68^\circ$ .

At the composition  $x = 0.52$  mol and at angle ( $2\theta$ ) of between  $42.5-47^\circ$ , there are 3 peaks (almost equal in height) representing one rhombohedral phase peak (center, blue line) for the (220) plane and at the left-right side representing the 2 tetragonal phase peaks (the yellow line) for the (020) and (002) planes. The presence of high-low peaks is determined from the content of each phase. So, it can be concluded that the value of x decrease, so the tetragonal phase contents increase.

As the piezoelectric solid materials which typically exhibit enhanced electromechanical properties are in compositions with a morphotropic phase boundary (MPB) separating the two phases of the crystal system with different polarization orientation indications. Therefore, XRD profiles analysis has been required in separation for each rhombohedral and tetragonal phase in determining the crystalline system and the quantity. As mentioned above, we have been able to identify the transformation or phase transition of the crystal system.



**Fig. 4** The diffraction patterns and data refinements of the synthesized results in variations of x for the rhombohedral phase (I rhombohedral, blue line) and tetragonal (I tetragonal, yellow line). The lobs (dot red line) is intensity of XRD data and I<sub>tot</sub> (red line) is the total refinement intensity of the combined rhombohedral and tetragonal.

Tetragonal and rhombohedral percentages which have been the output of the fitting process can clearly determine the position of the transition area of MPB as shown Fig. 5 indicates that the 50:50 position is at the position around  $x = 0.52$ . The decrease of tetragonal (94-8.8 %) and the increase of rhombohedral phase content (6-91.2 %) have occurred very sharply with increasing  $x = 0.42$  to  $0.58$  mole. Therefore, analysis of the results of the minimum c/a ratio (tetragonal phase) and the percentage of content between tetragonal and rhombohedral phase has been concluded that the area of MPB is at  $x = 0.52$  or with the composition of  $PbZr_{0.52}Ti_{0.48}O_3$ .

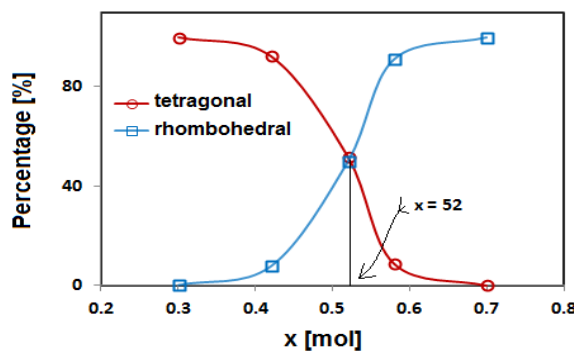


**Fig. 5** Percentage of refinement process results for tetragonal and rhombohedral phase contents.

Crystals defects can occur during the synthesis process, due to the formation of polycrystalline aggregations. This has an effect on deviations of perfect crystallinity so that it can lead to broad-narrow from the diffraction peaks. Crystallite size and lattice strain are two main characteristics that can be processed from the peak width analysis [18]. The size and strain can affect the peak broadening, and can be estimated with using Williamson-Hall's analysis method as a function broadening peak width and peak position  $2\theta$  [18-19]. The strain induced in powders due to crystal imperfection and distortion was calculated using the formula  $\epsilon = \beta / 4 \tan \theta$ , where  $\beta$  (full width at the half maximum, FWHM) was taken from the refinement results and  $\theta$  is the diffracted angle.

With this approach, Williamson-Hall plot is formulated and interpolated with the equations  $\beta \cos \theta = k\lambda/d + 4 \epsilon (\sin \theta)$ , and can also be illustrated as shown in Fig. 5. Where  $d$  is the crystallite

particle size,  $\epsilon$  elastic strain, and  $K$  is Scherrer constant (the somewhat arbitrary value that falls in the range 0.87–1.0. we usually assume  $k = 1$ ). Previously, XRD intensity profile of silicon samples as standard material has been used to correct the intensity and peak positions to determine FWHM (identical to peak broadening) in this refinement process, as performed by Engkir [20].

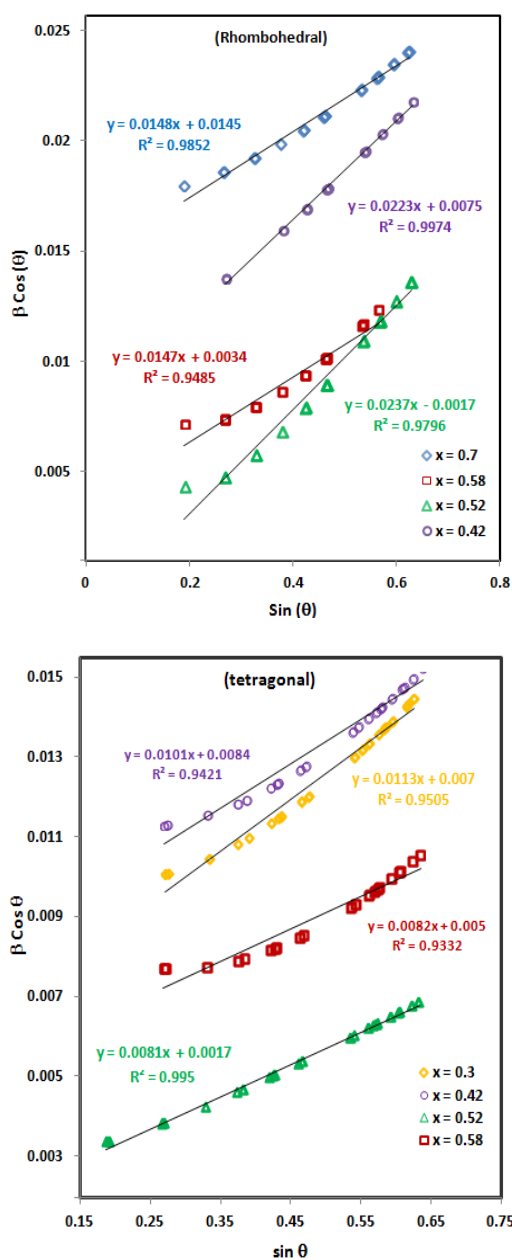


**Fig. 6** Williamson plots from the refinement results for rhombohedral and tetragonal phases with various compositions  $x$  in  $PbZr_xTi_{(1-x)}O_3$ .

To ensure that the size of the crystallite particles for each of the  $x$  compositions of the rhombohedral and tetragonal phases can be calculated using the Williamson-Hall plot, as shown in Fig. 6. Statistically, all R-squared values have been obtained above 93% which indicates good enough. Crystallite particle size can be calculated from the y axis -intercept of the fitted line. Importantly all the slope of the linear plots exhibit a positive value, that can interpret the size of crystallite particles, not imaginary.

Fig. 7 shows that the graph profile on the particle size is very identical for each phase. At the composition of  $x = 0.52$  the crystallite particle size of the rhombohedral and tetragonal phases shows the largest/maximum with almost equal values (906.117 Å), if  $x$  is varied from 0.3 to 0.7 mol. Macroscopically, the grain size of the synthesized powder has been seen using scanning microscope electron (SEM) equipment, as shown in the Fig. 8 below.

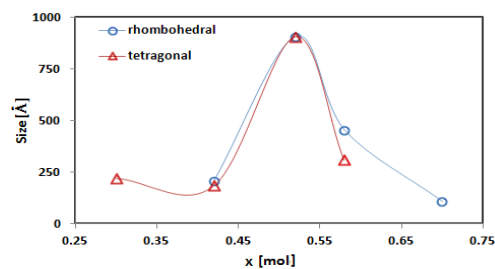


**Fig. 7** Graph of crystallite size against variation of composition  $x = 0.3, 0.42, 0.52, 0.58$  and  $0.7$  mol.

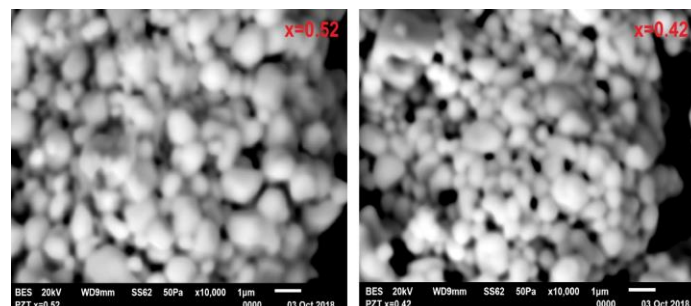


**Fig. 8** SEM micrographs on the results of PZT synthesis with  $x = 0.52$  and  $0.42$ .

SEM micrograph images (as shown in Fig. 8) clearly show that the particle size for  $x = 0.52$  is greater than  $x=0.42$ . The size of this particle is consistent with the analysis of the results of refinement of x-ray diffraction patterns, as mentioned above.

## CONCLUSION

Application of molten salt method on the synthesis of  $PbZr_xTi_{1-x}O_3$  materials has been successfully performed. There were two kinds of rhombohedral and tetragonal phases with each perovskite crystal system and having the MPB region (same quantity) at the composition  $x = 0.52$  mole. So, this has been the phase transition from tetragonal to rhombohedral which has been indicated by changes in x-ray diffraction peaks.

In this study, analysis of the results of the refinement process has shown that the crystallite particle size pattern has almost identical for each phase. While both with the largest size of about 906.117 Å is also at the composition  $x = 0.52$  mole.

## ACKNOWLEDGEMENT

I am very grateful to Dr. Abu Khalid (the head of BSBM-PSTBM, BATAN), Mr. Gunawan, and Dr. Mykel Manawan for initial work and scientific discussion. I would like to thank Mr. Iwan Setiawan and Mr. Jedgia Ginting for guiding the technical discussions in completing the laboratory works.

## REFERENCES

- [1] S. Zhang, R. Xia, T. R. Shrout, "Lead-free piezoelectric ceramics vs. PZT?," *J. Electroceram.*, vol. 19, no. 4, pp. 251 - 257, 2007.
- [2] K. Nagata, J. Thongrueng, "Effect of temperature, humidity and load on degradation of multilayer ceramic actuator," *J. Korean Phys. Soc.*, vol. 32, pp. S1278–S1281, 1998.
- [3] L. Medvecký, M. Kmecová, K. Saksli, "Study of  $Pb(Zr_{0.53}Ti_{0.47})O_3$  solid solution formation by interaction of Perovskite phases," *J. Eur. Ceram. Soc.*, vol. 27, no. 4, pp. 2031–2037, 2007.
- [4] C. A. Randall, N. Kim, J.-P. Kucera, W. Cao, T. R. Shrout, "Intrinsic and extrinsic size effects in fine-grained morphotropic-phase-boundary lead zirconate titanate ceramics," *J. Am. Chem. Soc.*, vol. 81, no. 3, pp. 677–688, 1998.
- [5] S. Ahda, S. Misfadhila, T. Y. S. P. Putra, P. Parikin, "Molten salt synthesis and structural characterization of  $BaTiO_3$  nanocrystal ceramics," *IOP Conf. Ser. Mater. Sci. Eng.*, vol. 176, 2017.
- [6] J. T. Zeng, K. W. Kwok, H. L. W. Chan, " $K_xNa_{1-x}NbO_3$  powder

- synthesized by molten-salt process,” *Mater. Lett.*, vol. 61, no. 2, pp. 409–411, 2007.
- [7] Y. Haibo, Y. Lin, F. Wang, H. Luo, “Chemical synthesis of  $K_{0.5}Na_{0.5}NbO_3$  ceramics and their electrical properties,” *Mater. Manuf. Process.*, vol. 23, no. 5, pp. 489–493, 2008.
- [8] N. Sharma, A. Gaur, U. Gaur, “Multiferroic behavior of nanocrystalline  $BaTiO_3$  sintered at different temperatures,” *Ceram. Int.*, vol. 40, no. 10 Part B, pp. 16441–16448, 2014.
- [9] F. Zhang, L. Han, S. Bai, T. Sun, T. Karaki, M. Adachi, “Hydrothermal synthesis of (K,Na)NbO<sub>3</sub> particles,” *Jpn. J. Appl. Phys.*, vol. 47, no. 9, pp. 7685–7688, 2008.
- [10] H. K. Yoon, Y. S. Cho, D. H. Kang, “Molten salt synthesis of lead based relaxors,” *J. Mater. Sci.*, vol. 33, no. 12, pp. 2977–2984, 1998.
- [11] J. Joseph, T. Vimala, V. Sivasubramanian, V. Murthy, “Structural investigations on  $Pb(Zr_xTi_{1-x})O_3$  solid solutions using the X-ray Rietveld method,” *J. Mater. Sci.*, vol. 35, no. 6, pp. 1571–1575, 2000.
- [12] H. Yokota, N. Zhang, A. E. Taylor, P. A. Thomas, A. M. Glazer, “Crystal structure of the rhombohedral phase of  $PbZr_{1-x}Ti_xO_3$  ceramics at room temperature,” *Phys. Rev. B*, vol. 80, pp. 104109, 2009.
- [13] A. Chauhan, P. Chauhan, “Powder XRD technique and its applications in science and technology,” *J Anal Bioanal Tech* vol. 5, no. 5, 2014.
- [14] O. Namsar, A. Watcharapasorn, S. Jiansirisomboon, “Fabrication and characterization of PZT/nano-sized  $Si_3N_4$  ceramics,” *J. Microsc. Soc. Thail.*, vol. 23, no 1, pp. 103–106, 2009.
- [15] C. T. Kniess, J. C. de Lima, P. B. Prates, The quantification of crystalline phases in materials: Applications of Rietveld method, sintering - Methods and products, Volodymyr Shatokha (Ed.), IntechOpen. 2012.
- [16] N. Sahu, S. Panigrahi, “Mathematical aspects of Rietveld refinement and crystal structure studies on  $PbTiO_3$  ceramics,” vol. 34, no. 7, pp. 1495–1500, 2011.
- [17] A. S. Karapuzha, N. K. James, H. Khanbareh, S. van der Zwaag, W. A. Groen, “Structure, dielectric and piezoelectric properties of donor doped PZT ceramics across the phase diagram,” *J. Ferroelectr.*, vol. 504, no. 1, pp. 160–171, 2016.
- [18] Y. T. Prabhu, K. V. Rao, V. S. S. Kumar, B. S. Kumari, “X-ray analysis by Williamson-Hall and size-strain plot methods of ZnO nanoparticles with fuel variation,” *World J. Nano Sci. Eng.*, vol. 04, no. 1, pp. 21–28, 2014.
- [19] C. Suryanarayana, M. G. Norton, X-ray diffraction: A practical approach. New York: Springer, 1998.
- [20] E. Sukirman, Y. Sarwanto, “X-rays diffraction study on the iron nanoparticles prepared by two step milling method,” *J. Sains Mater. Indones.*, vol. 15, no. 2, p. 67, 2014.